Proceedings of ASME Turbo Expo 2011
GT2011
June 6-10, 2011, Vancouver, British Columbia, Canada

GT2011-45633

ENGINE PARAMETER ESTIMATION IN TEST CELLS USING HYBRID PHYSICS/EMPIRICAL MODELS

Jonathan A. DeCastro
Impact Technologies, LLC
Rochester, NY 14623

Dean K. Frederick
Saratoga Control Systems, Inc.
Saratoga Springs, NY 12866

Liang Tang
Impact Technologies, LLC
Rochester, NY 14623

ABSTRACT

Estimation of engine parameters such as thrust in test cells is a difficult process due to the highly nonlinear nature of the engine dynamics, the complex interdependency of thrust and the engine's health condition, and factors that corrupt thrust measurements due to test stand construction. Because the frequency content of the corrupting dynamics is close to the engine's dynamics, filtering the thrust signal is not sufficient for extraction of the true dynamic content. A configurable thrust estimation system is developed for accurate data reduction which provides "virtual" measurements of thrust and other necessary parameters at steady state and during aggressive engine transients. The thrust estimation framework consists of a representative nonlinear engine model coupled with an adaptive structural dynamics model. To account for discrepancies between the physics-based model and the true engine, a hybrid model using a novel neural network (NN) enhancement to a physics-based engine model is presented that reduces certain modeling errors between the engine model and the physical plant. This includes engine-to-engine variation, engine degradation and any essential neglected dynamics. To fuse the model and sensor measurements, this hybrid model is used within a constant-gain extended Kalman filter batch estimator which is able to reconstruct the true dynamic performance of the engine using noisy or corrupted sensor measurements and control inputs. The Kalman filter estimates measured and unmeasured parameters and state variables such as engine component deterioration parameters and effective flow areas.

INTRODUCTION

Owing to the strict demands on performance, the certification process for military engines is highly involved because of the severe operational maneuvers and transients that will be encountered during combat. Millions of dollars are spent on acceptance testing of military engines to examine thrust ratings, transient response, thrust specific fuel consumption (TSFC), etc. The costs and duration of these tests ultimately impact the cost-of-ownership and availability of the engine fleet [2]. During typical testing, transient test data exceeding 40 terabytes is collected for post-processing, performance evaluation, model-building, and controls development. These acceptance tests are therefore extremely expensive to operate. Since the availability of engine components is critical for the maintenance and readiness of the fleet, the value of a more streamlined method to acquire data for characterizing the dynamic and transient performance characteristics would be very desirable.

In a test cell environment, the measurements are subject to vibrations which render data collection an error-prone task. In certain test stands, the natural vibration modes are low enough for excitations produced by the thrust output couple into the test stand and dominate the signal. Since transient data is often needed for performance data reduction, stand-induced vibrations can completely obfuscate the engine's actual transient characteristics. To confound matters, load cell data is not always available or may be contaminated badly enough that the operator deems it necessary to ignore the results. Because the engine data is convoluted with test stand dynamics, it is not feasible to simply filter the thrust signal. It is possible to instead use models, along with other engine measurements to aid in reconstructing the true transient character of the engine. An accurate, adaptable thrust estimation scheme will therefore be of great value to the certification process and will save the industry millions of dollars in certification costs.

Indeed, modern engine control systems do not presently use a thrust estimate as the feedback variable because of the difficulty of correctly estimating that variable. When estimating thrust, particular attention has to be paid to estimating health parameters accurately, a task that becomes even more difficult when there are a limited number of sensors available to form the estimate [7]. The highly nonlinear nature of the engine dynamics and the complex dependency of thrust on the engine's health condition further increase these difficulties. The methodology developed by Volponi [11] uses a state variable model in conjunction with a Kalman filter and neural network to correctly estimate parameters. The Kalman filter used in that work was based on piecewise linear models and the neural network was designed at the outputs of the system. Our case, in contrast, requires exploration of methodologies that make *explicit use of a high-fidelity engine model* and use an empirical modeling element that provides value even for outputs which are *excessively noisy or altogether absent*.

High-fidelity engine models have been developed to perform cycle performance analysis for the purposes of engine and control system design. Examples include the Numerical Propulsion System Simulation (NPSS) code [4], the Modular Aero-Propulsion System Simulation (MAPSS) [8], and the Commercial Modular Aero-Propulsion System Simulation (C-MAPSS) [1], all developed by NASA. NPSS models are typically available for new engines that are under development, and thus are powerful tools from which to develop an effective thrust estimation system. More computationally-efficient models are also being developed, such as that by Frederick [2] which can accurately describe engine operation to a reasonable degree of accuracy.

In this paper, a thrust estimation scheme is presented to provide "virtual" measurements of thrust and other parameters of interest that are true to the actual engine, even during aggressive engine transients. To capture any discrepancies between the physics-based model and the true engine, a Neural Network (NN) is used to reduce any errors between the nonlinear model and the physical plant. The NN removes the variability in the engine model due to engine-to-engine variation and engine degradation. This hybrid empirical/physics model will then be used within a Kalman filter estimator structure that will be able to reconstruct the true dynamic performance of the engine using noisy or corrupted sensor measurements and control inputs.

The algorithm is configurable to many engine platforms, and the developed software allows for generation of embeddable nonlinear engine models for the thrust estimation scheme. Furthermore, the developed software enables generation of tuned hybrid models of the engine, which have been validated against actual data. Optionally, the parameterized models can be extracted from the estimator and used directly in controls design. To demonstrate the thrust estimator strategy, simulation results using the NASA Modular Aero-Propulsion System Simulation (MAPSS) engine model are reported. Test cases at sea-level static and simulated altitude/speed conditions reveal promise for the methodology in extracting an accurate, validated thrust output. It is envisaged that the model can be interchanged with any dynamic cycle deck model that is available for a given engine platform, such as the Numerical Propulsion System Simulation (NPSS).

NOMENCLATURE

A, B, C, D, L, H	System matrices (Jacobians)
EKF	Extended Kalman filter
Fn	Net thrust
h	Deterioration (health) parameter vector
HPC	High-pressure compressor
HPT	High-pressure turbine
K	Kalman gain matrix
LPC	Low-pressure compressor (booster)
LPT	Low-pressure turbine
MAPSS	Modular Aero-Propulsion System Simulation
N1	LP spool (fan) speed
N2	HP spool (core) speed
NN	Neural network
PCNfR	Percent corrected fan speed
PLA	Power lever angle
Q	Process covariance matrix
R	Measured output covariance matrix
SLS	Sea-level static
TMPC	Spatially-averaged metal heat soak temperature
u	Input vector
v	Measurement noise vector
w	Process noise vector
Wf	Fuel flow rate
x	State vector
x_m	Measured portion of the state vector
x_u	Unmeasured portion of the state vector
y	Measured output vector
z	Unmeasured output vector
ϕ	Component flow capacity
η	Component efficiency

SEMI-EMPIRICAL NONLINEAR ESTIMATION APPROACH

The basic model required to predict the engine states follows a standard nonlinear process that contains both measured and unmeasured outputs. Considering the engine system

$$\begin{aligned} \dot{x} &= f(x,h,u) \\ y &= g_m(x,h,u) \\ z &= g_u(x,h,u) \end{aligned} \tag{1}$$

where *x* is the state vector, *u* is the input vector, *h* is the vector of deterioration parameters, *y* is the measured output vector, and *z* is the unmeasured output vector. The vector *z* may contain variables such as thrust and compressor stall margins. The estimation structure is designed to estimate the unmeasured variable *z* via estimates of *x* and *h* using *u* and *y*. To be representative of an engine mounted in a test stand, the process model is composed of a nominal engine model obtained as described by a high-fidelity numerical simulation coupled with a structural model that is assumed unknown. For the purposes of this paper, the structural model introduces unmodeled dynamics that prevent accurate measurements of engine thrust to be made. The diagram in Figure 1 shows the overall structure of the semi-empirical estimator.

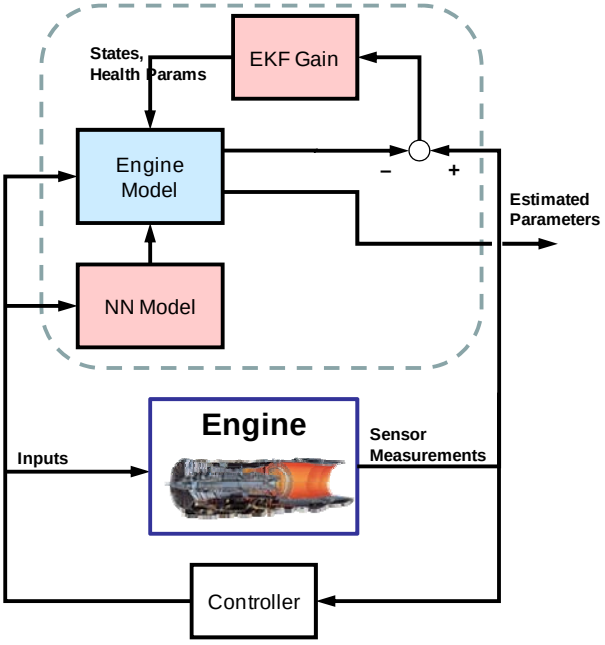

Figure 1. Structure of the thrust estimation system.

Empirical Model

Since engine models usually do not match the actual engine under test, an empirical engine model is used in this work to supplement the nominal physics-based model. In this case, a neural network was used to approximate the dynamics in Eq (1) using a novel approach which learns mismatches in the model by training on processed versions of select engine measurements. This has a particular advantage in thrust estimation. Because it is often impossible to guarantee a dynamically un-corrupted measurement of thrust, learning modeling mismatches between measured and modeled thrust can significantly impair the estimation approach if the empirical model absorbs the corrupting dynamics. To accommodate this, the present modeling method appropriately modifies the engine dynamics based on a subset of the more reliable, relatively low-noise sensor measurements. The result is an empirical model that improves the dynamic and steady-state matching in the thrust output with respect to the nominal physical model, and improves matching in most other outputs as well. The methodology has been verified through simulation, where the ground truth is known. Due to the proprietary nature of this technique, further details of the implementation are omitted.

Extended Kalman Filter

To make direct use of the full engine model, and also reduce the computational burdens brought about by the traditional extended Kalman filter (EKF), a variation on the EKF is used here. The Constant-Gain Extended Kalman Filter (CGEKF) is a technique introduced by Safanov and Athans [9] for nonlinear estimation using an implicit (high-fidelity) model. Sugiyama [10] and Kobayashi, Simon and Litt [6] implemented the procedure for engine parameter estimation. In this filter, the Kalman gain *K* is a constant matrix designed at a representative operating point based on the following linearized open-loop engine model:

$$\begin{aligned} \delta\dot{x} &= A\delta x + L(h-1) + B\delta u + w_1 \\ \dot{h} &= w_2 \\ \delta y &= C_y\delta x + H_y(h-1) + D_y\delta u + v_1 \\ \delta z &= C_z\delta x + H_z(h-1) + D_z\delta u + v_2 \end{aligned}$$

where

$$\begin{aligned} \delta x &= x - x_{ss} \qquad \delta u = u - u_{ss} \\ \delta y &= y - y_{ss} \qquad \delta z = z - z_{ss} \end{aligned}$$

and where the subscript "*ss*" refers to the steady-state condition at which the Kalman filter is designed. *x* is the vector of engine states, *u* is the vector of control inputs and environmental inputs, *y* is the vector of measured outputs and *h* is the vector of health parameters. In the above implementation, *h* – 1 is meant to represent the deviation from nominal. The outputs are hence described by a linear combination of the states, health parameters, engine inputs, and noise. The Jacobians *A*, *B*, *C*, *D*, *L*, and *H* are numerically obtained from the process and measurement equations. The estimator is implemented using the following process:

$$\begin{Bmatrix} \dot{\hat{x}} \\ \dot{\hat{h}} \end{Bmatrix} = \begin{bmatrix} \hat{f}(\hat{x},\hat{h},u) \\ 0 \end{bmatrix} + K(y - g_y(\hat{x},\hat{h},u))$$

where $\hat{f}(\hat{x}, \hat{h}, u)$ contains both the nominal nonlinear engine model and the empirical model. Ref. [9] proved the conditions under which this class of nonlinear observers with constant gain matrix *K* is non-divergent.

In the CGEKF formulation, the first moment (mean) is propagated through the nonlinear process equation, while the covariance is only propagated through a static relationship valid for the linear case. Because of this statistical approximation, the filter is suboptimal. Note that, while the Safanov and Athans version of the filter uses an affine representation of the system, the one used here does not necessarily require such structure. Because of this, the covariances *Q* and *R* no longer hold statistical meaning but (as in Refs. [10] and [6]) are instead treated as free design parameters.

THRUST ESTIMATION USING MAPSS

The MAPSS military engine model [8] and fan-speed control system is used in this work as both the truth model and the estimator model. The MAPSS model operates at a 0.02-sec step size and was altered to include easy access to deterioration parameters, addition of the closed-loop control system, addition of system sensors, and addition of sensor noise. The list of inputs and states in the MAPSS model for sea-level, static (SLS), standard-day operation are shown in Table 1.

Table 1. State and auxiliary variables for the MAPSS engine model.

	Designation	Variable Description
Pilot Input	PLA	Power lever angle (deg.)
Controller Output	Wf36	Primary fuel flow rate (lbf/hr)
Engine State Variables	N1	Fan speed (rpm)
	N2	Core speed (rpm)
	TMPC	Average heat soak temperature (°R)

Engine Sensors. The sensors under consideration in the MAPSS model are given in Table 2. Note that thrust is included in the list, with the understanding that the thrust sensor would be part of the test cell mounting, rather than on the engine itself. A set of first-order sensor models having unity DC gain represent sensor dynamics. Sensor noise was adapted from a noise model obtained from NASA. The noise is assumed to be zero-mean colored noise, constructed by passing Gaussian-distributed noise, with variance that is proportional to the signal's current value, into a low-pass filter with a small time constant. The resulting pre-filtered noise standard deviations are shown in Table 3. The thrust sensor (test stand-mounted load cell) has more complicated dynamics and is described in greater detail later in the section.

Table 2. Sensed variables for the MAPSS engine model.

Index	Designation	Sensed variable
1	N1	Fan speed (rpm)
2	N2	Core speed (rpm)
3	Fn	Net thrust (lbf)
4	Ps21	Fan exit static pressure (psia)
5	P27D	Duct stream pressure (psia)
6	T27D	Duct stream temperature (°R)
7	P27	Core stream pressure (psia)
8	T27	Core stream temperature (°R)
9	T3	HPC exit temperature (°R)
10	Ps15	Bypass duct static pressure (psia)
11	P16	Bypass mixing plane pressure (psia)
12	Ps3	Bleed static pressure (psia)
13	T5B	LPT blade temperature (°R)
14	T56	LPT temperature (°R)
15	Ps56	Mixer static pressure (psia)
16	P58	Mixer pressure (psia)

Table 3. Sensor noise standard deviations for each sensor.

Sensor	Standard deviation, σ	Unit
N1	28.61	rpm
N2	37.77	rpm
Fn	1000	lbf
Ps21	0.145	psia
P27D	0.176	psia
T27D	5.272	°R
P27	0.187	psia
T27	5.262	°R
T3	10.274	°R
Ps15	0.273	psia
P16	0.276	psia
Ps3	1.335	psia
T5B	14.995	°R
T56	19.715	°R
Ps56	0.252	Psia
P58	0.263	Psia

Engine Deterioration. Deterioration inputs were added to all five rotating components (Fan, LPC, HPC, HPT, and LPT). The deterioration level of each rotating component can be specified, producing the desired efficiency and flow modifiers for each component. Table 4 shows the deterioration parameter designations for each rotating component. For the purposes of demonstration, the percentage change in flow capacity and efficiency is directly proportional to the deterioration parameter.

Table 4. Deterioration parameters for each of the five rotating components.

Parameter	Description
$h_{\mathrm{Fan}}(=\Delta\phi_{\mathrm{Fan}}=\Delta\eta_{\mathrm{Fan}})$	Fan deterioration modifier
$h_{\mathrm{LPC}}(=\Delta\phi_{\mathrm{LPC}}=\Delta\eta_{\mathrm{LPC}})$	LPC deterioration modifier
$h_{\mathrm{HPC}}(=\Delta\phi_{\mathrm{HPC}}=\Delta\eta_{\mathrm{HPC}})$	HPC deterioration modifier
$h_{\mathrm{HPT}}(=\Delta\phi_{\mathrm{HPT}}=\Delta\eta_{\mathrm{HPT}})$	HPT deterioration modifier
$h_{\mathrm{LPT}}(=\Delta\phi_{\mathrm{LPT}}=\Delta\eta_{\mathrm{LPT}})$	LPT deterioration modifier

Closed-Loop Controller. A fan-speed controller with gains scheduled for SLS, standard-day conditions is applied to the MAPSS model, along with a power management table to convert from user-specified values of PLA to percent corrected fan speed (PCNfR), from which the demanded fan speed can be computed. The designed controller is able to accommodate a PLA range between 20 and 50 degrees, which is the range of "dry" operation (no afterburning).

Thrust Measurement and Test Stand Dynamics. The main difficulty with test cell measurements is that the test stand is dominated by structural modes that corrupt the thrust measurement. In addition, flow-induced noise is present, producing oscillations that further corrupt the measurement.

In an attempt to provide a representative evaluation of heavily-corrupted test cell measurements, a simple yet representative model of the test stand has been developed to conceptually prove the estimation methodology. Based on an assumption that the structural modes in the test stand are lightly-damped with a dominant 3-Hz frequeency, the model consists of a second-order longitudinal model, as shown in Figure 2. By modeling the system as a lightly-damped first-order (single-mode) system, it is possible to generate a response that is fairly representative of the low-frequency system response (below 10 Hz). A more representative model will be necessary, however, to do more advanced evaluations of more complicated thrust measurements (e.g. vectored thrust in all 6 axes).

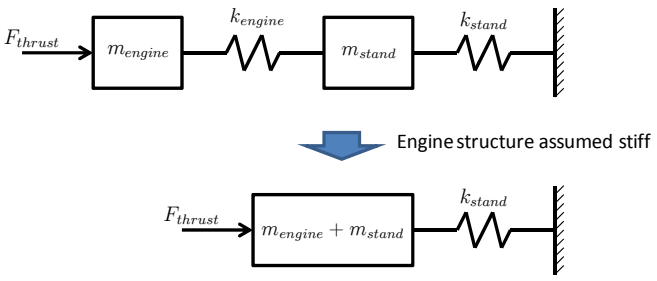

Figure 2. Single-mode model of test stand (longitudinal direction).

The simplified test stand dynamics are incorporated into the resulting model shown in Figure 3. Since the output core stream is dominated by noise, the pressure pulsations were replicated via experimental frequency spectra obtained from the literature. One example of a near-field noise spectrum is as found in Harper-Bourne [4]. Here, each of the pressure spectra are functions of the jet velocity. Both hydrodynamic and mixing noises are prominent at low frequencies, while shock noise is prominent at high frequencies, well out of the frequency range of measureable interest (i.e. thrust measurement sample rate). To implement the near-field pressure spectrum we have fitted a subset of these spectra below 1000 Hz and extrapolated to generate a response down to 1 Hz. As shown in the figure, this spectrum is added to the MAPSS engine output and fed into the structural model. At the output of the structural model, this is summed with the sensor noise process. The resulting noisy thrust signal is shown in Figure 4.

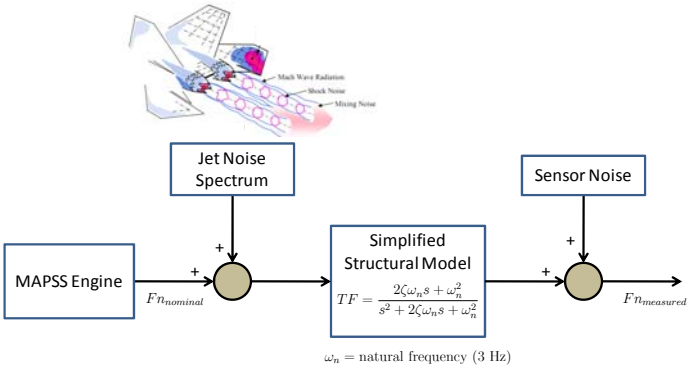

Figure 3. Thrust measurement model to be used for evaluation of uni-axial thrust estimation scheme.

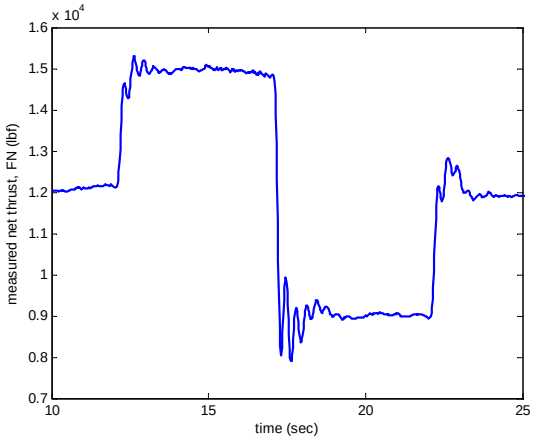

Figure 4. Example of measured thrust to a PLA doublet.

SIMULATION RESULTS

In this section, the results of the estimation methodology are presented. To design the Kalman filter, the *Q* matrix is taken as a diagonal matrix with dimension equal to the number of states to be estimated. In MAPSS, *Q* is 8x8, since the augmented state vector contains the engine states plus the deterioration parameters. The *R* matrix is also diagonal with dimension equal to the number of sensors available for measurement. For the CGEKF design, the process/measurement noise variances are as shown in Table 5.

In all the cases explored in this paper, modeling disparities are represented by introducing a mismatch in engine health coupled with some modeling mismatch. As indicated earlier, shifts in deterioration parameters can be representative of engine-to-engine mismatch, faults, and degradation. To represent the modeling mismatch in this study, a bias is applied to the power extraction on the high-pressure (HP) shaft to represent an unknown modeling mismatch, which introduces significant variability in the response.

Table 5. Kalman filter process and measurement noise variances.

State	Covariance (Q)	Sensor	Covariance (R)
x1 (N1)	2	N1	11444
x2 (N2)	2	N2	15108
x3 (TMPC)	2	Fn	166720
x4 (h_{Fan})	2	Ps21	28.911
x5 (h_{Bst})	20	P27D	35.124
x6 (h_{HPC})	2	T27D	702.93
x7 (h_{HPT})	2	P27	37.314
x8 (h_{LPT})	2	T27	701.63
		T3	1369.9
		Ps15	54.500
		P16	55.223
		Ps3	267.07
		T5B	1999.3
		T56	2628.7
		Ps56	50.333
		P58	52.668

Kalman Filter Performance With Thrust Measurement

To evaluate the Kalman filter engine parameter estimation, several runs were made at various power settings at sea-level, static, standard-day conditions. The deterioration parameters are set to 4%, corresponding to an engine with severe degradation with respect to some nominal healthy condition. A power extraction mismatch of 1500 W is introduced to represent model-plant mismatch. A PLA doublet of magnitude 6 degrees is introduced, with the first upswing occurring at 2 seconds, downswing at 7 seconds, and second upswing at 12 seconds. The results for an initial PLA of 40 degrees is shown in Figure 5, Figure 6, and Figure 7. Figure 5 reveals the activity of the Kalman estimator attempting to compensate for the modeling discrepancies through adjustment of health parameters. As shown in Figure 6, the three states are all accurately estimated and the first eight sensors in the list in Table 2 are correctly estimated (the remaining eight are omitted for conciseness). For all sensor outputs, the estimated responses are much closer to the actual values than using the model alone. In steady-state, the mismatch between the model and engine produces a 340 lbf (about 6%) discrepancy in thrust. A close-up of the thrust estimate during the doublet downswing (Figure 7) shows that the estimator captures some of the unwanted oscillatory behavior of the test stand dynamics. Better steady-state matching can be made by increasing the weight of the *Q* matrix relative to the *R* matrix, but this comes at the penalty of increasing the oscillatory response of the estimate.

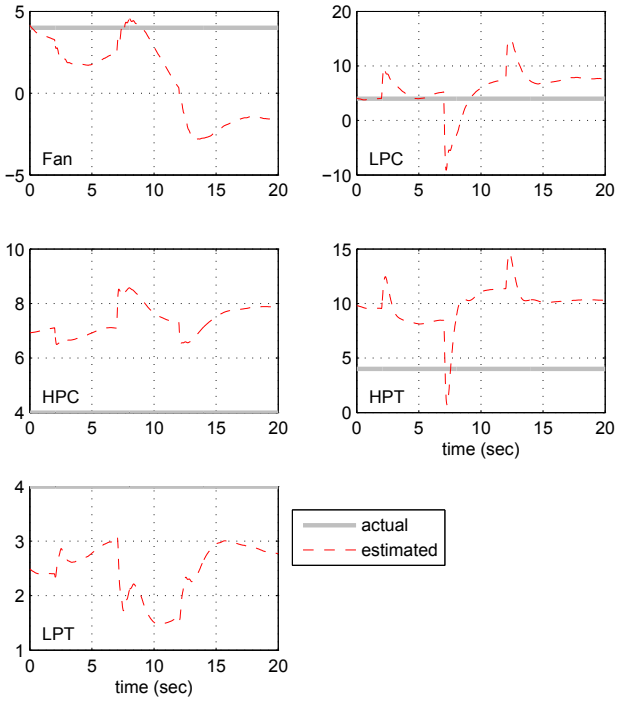

Figure 5. Actual component deteriorations (health parameters) plotted against estimated values with engine degradation for a 10-deg PLA step applied at 10 seconds.

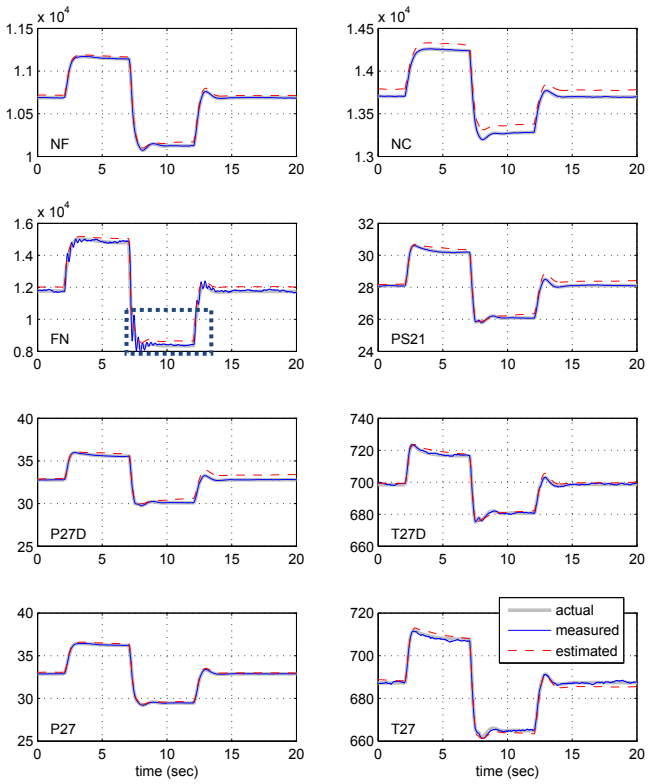

Figure 6. Measured sensor outputs plotted against estimated values with engine degradation for a 6-deg PLA doublet.

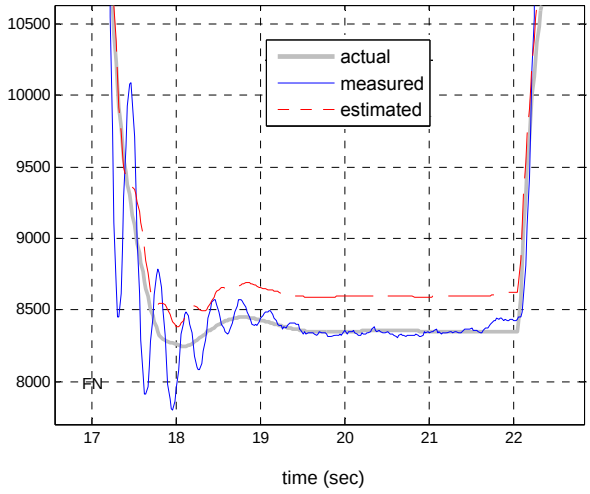

Figure 7. Close-up of thrust estimate along with noisy thrust measurement (boxed region in Figure 6).

Kalman Filter Performance Without Thrust Measurement

For the case where thrust measurements are not available, the thrust estimator only has 15 sensors at its disposal. Again considering the setting PLA = 40 degrees with 4% deteriorations on all components and a power extraction mismatch of 1500 W, the result is a steady-state mismatch in net thrust of 650 lbf, an inaccuracy of 5.5%. Time histories using the same input profile as the previous case are shown in Figure 8. Other parameters deviate similarly to the case with thrust measurement. Although this result underscores the importance of the thrust measurement to eliminate steady-state errors, the thrust dynamics can be accurately reconstructed with the remaining sensors, provided they are corrupted only with a nominal amount of noise.

The results show that the parameter estimation scheme is functioning well, *both with and without thrust estimates*, and is well-suited to handle gross mismatches between the engine and model. Based on the runs made, the thrust parameter is well-estimated, and does not deviate much even with large shifts in health parameters and high-pressure spool power extraction (to simulate engine mis-modeling). Nonetheless, variability may be found as different operating conditions are encountered, and the actual application may exhibit more modeling variability than was contemplated in these simulations. Therefore, the empirical modeling component can be a critical piece of the overall estimation structure.

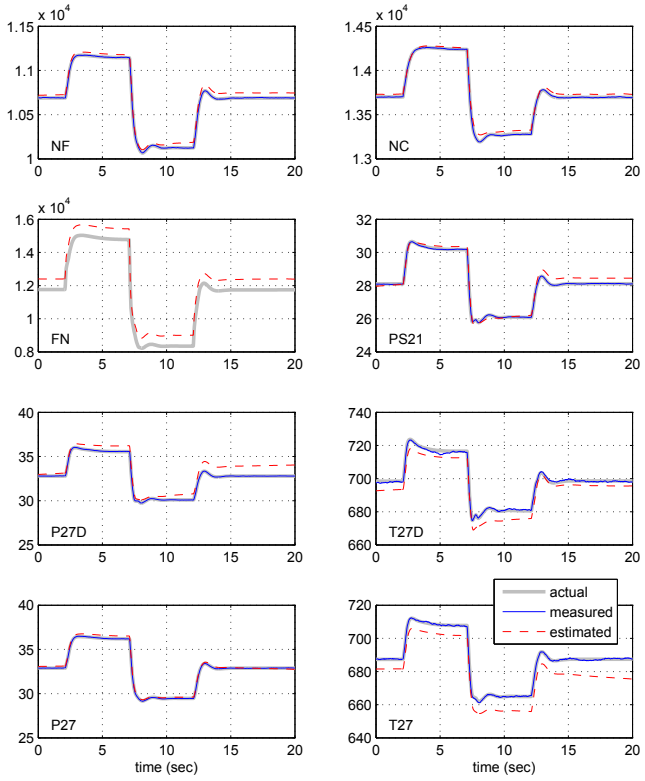

Figure 8. Measured sensor outputs plotted against estimated values with engine degradation and power extraction for a 6-deg PLA doublet. Estimator designed without thrust sensor.

CONCLUSIONS AND FUTURE WORK

In this paper, an estimation methodology is presented that makes use of a high-fidelity nonlinear model coupled with an empirical model to estimate measured and unmeasured parameters. This method is under development for a test stand application for use where mere filtering of the thrust signal is not a viable option; e.g. when the frequency range of the test stand dynamics overlaps (and hence contaminates) the dynamics of the engine process. The empirical component of the model aims at reducing model-plant mismatches arising from process model uncertainties that are not necessarily (or completely) attributable to health parameter mismatches. The Kalman filter estimator is used to further reduce errors by manipulating estimates of engine states and health parameters. The approach is particularly suited for performance data reduction using engine test stand instrumentation which is corrupted with noise and whose thrust measurements dominated by test stand structural dynamics. As indicated by simulation studies conducted on the MAPSS engine model, the estimator improves the capability to provide estimates of unmeasured engine outputs both in steady-state and transient operation.

Two important features define the methodology. Firstly, since this is an off-board estimator, the requirement is to make *direct* use of nonlinear engine models which are more accurate in making predictions of the engine's behavior than their piecewise linear counterparts for model-building, identification, and certification. The approach therefore uses a Kalman filter based on an intrinsic internal model. The second feature is the requirement to make use of empirical modeling work well with unmeasured (or highly corrupted) engine outputs such as thrust. In this paper, a novel method for empirical modeling is presented. This is shown to improve the dynamic and static response of the states as well as estimates of the thrust output.

In this study, only the uni-axial thrust component was considered and a model of thrust noise-induced vibrations was incorporated within the evaluation framework to simulate the actual environment. It is possible to include models of vectored thrust nozzles to determine the reaction forces on 6-axis-measurement test stands. NPSS models typically contain more detailed effects such as these, as well as use of customized inlets used in test cells. Porting the methodology to the NPSS realm will not only ensure applicability across a wide range of engine platforms and configurations, but also aid in streamlining the development cycle of new engines and control systems. The continuation of this effort will also focus on incorporating a model of the test stand dynamics directly into the filter structure. With the inclusion of the test stand dynamics in the formulation, the dynamics can be estimated by the filter and thus estimates of unmeasured thrust may improve. If necessary, unknown parameters such as the dominating natural frequencies, can be modified through an adaptation mechanism.

ACKNOWLEDGMENTS

The authors gratefully acknowledge the support of the Navy SBIR program and also that of program monitor Glen Karlsons of NAVAIR. The contributions of Dr. Al Volponi, Bruce Wood, Bill Gallops, and Dr. Ravi Rajamani from Pratt & Whitney are greatly appreciated.

REFERENCES

[1] DeCastro, J.A., Litt, J.S. and Frederick, D.K., 2008, "A Modular Aero-Propulsion System Simulation of a Large Commercial Aircraft Engine", Proceedings of the 44th AIAA/ASME/SAE/ASEE Joint Propulsion Conference & Exhibit, Hartford, CT, 21–23 July 2008.

[2] Federal Aviation Administration (FAA), 2002, "Correlation, Operation, Design and Modification of Turbofan/Jet Engine Test Cells," FAA Advisory Circular, No. 43-207, December.

[3] Frederick, D.K., 2009, "A New Method for Constructing Fast Models of Jet Engines in Simulink," Proceedings of the 45th AIAA/ASME/SAE/ASEE Joint Propulsion Conference & Exhibit, Denver, CO, 2-5 August, 2009.

[4] Harper-Bourne, M., 2001, "Predicting the Jet Near-Field Noise of Combat Aircraft," Presented at the RTO AVT Symposium on Ageing Mechanisms and Control: Part A – Developments in Computational Aero- and Hydro-Acoustics, Manchester, UK, 8-11 October 2001.

[5] Jones, S.M., 2007, "An Introduction to Thermodynamic Performance Analysis of Aircraft Gas Turbine Engine Cycles Using the Numerical Propulsion System Simulation Code," NASA/TM—2007-214690.

[6] Kobayashi, T., Simon, D.L., and Litt, J.S., 2005, "Application of a Constant Gain Extended Kalman Filter for In-Flight Estimation of Aircraft Engine Performance Parameters," ASME Paper No. GT2005–68494.

[7] Litt, J.S., 2005, "An Optimal Orthogonal Decomposition Method for Kalman Filter-Based Turbofan Engine Thrust Estimation," NASA/TM—2005-213864 (ARL–TR–3487 and ASME Paper GT2005–68808).

[8] Parker, K.I., Guo, T.H., 1978, "Development of a Turbofan Engine Simulation in a Graphical Simulation Environment," NASA/TM-2003-212543.

[9] Safonov, M.G. and Athans, M., 1978, "Robustness and Computational Aspects of Nonlinear Stochastic Estimators and Regulators," *IEEE Transactions on Automatic Control*, Vol. AC-23, No. 4, pp. 717–725.

[10] Sugiyama, N., 2000, "System Identification of Jet Engines," *J. Engineering for Gas Turbines and Power*, Vol. 122, No. 1, pp. 19-26.

[11] Volponi, A., 2008, "Enhanced Self Tuning On-Board Real-Time Model (eSTORM) for Aircraft Engine Performance Health Tracking," NASA Contractor Report, NASA/CR-2008-215272.